CHEMISTRY OF MATERIALS
Article

Chem. Mater. **2009,** *21,* 4589–4597 4589
DOI:10.1021/cm9016535

Mesostructured Hybrids Containing Potential Donors and Acceptors with Molecular-Scale and Meso-Scale Segregation and Ordering: Toward the Development of Smart Materials through Hierarchical Self-Assembly

Le-Le Li,[†] Hao Sun,[†] Chen-Jie Fang,[‡] Quan Yuan,[†] Ling-Dong Sun,[†] and Chun-Hua Yan*,[†]

[†]*Beijing National Laboratory for Molecular Sciences, State Key Lab of Rare Earth Materials Chemistry and Applications & PKU−HKU Joint Lab in Rare Earth Materials and Bioinorganic Chemistry, Peking University, Beijing 100871, China, and* [‡]*School of Pharmaceutical and Chemical Biology, Capital Medical University, Beijing 100069, China*

Received June 15, 2009. Revised Manuscript Received August 31, 2009

A novel self-assembly approach was developed to design and synthesize innovative mesostructured hybrid materials with intimately contacted potential donor (**D**) and acceptor (**A**) domains organized in a three-dimensional ordering. Two specific organic and inorganic components, both of which bear optoelectronic functionalities (**D** and **A**, respectively), were designed and used. Then the one-step self-assembly process locks both **D** and **A** molecules into ordered three-dimensional nanostructure, which may allow for the uniform and molecular level controllable organization of the **D** and **A** molecules in the central regions of the pore channels and the pore walls of the hybrids, respectively. The optical properties were discussed in relation to the architectures of the materials, which offer an opportunity to disclose the distribution model of organic molecules within the mesostructured hybrids. Obviously, this hierarchical self-assembly of advanced architectures indicates that it should readily be possible to substitute the **D** and **A** for alternative different functional groups, which is of great importance toward the development of a family of smart materials for the purpose of constructing novel platforms for field effect transistors, solar cells, and other device applications.

Introduction

Over the past decades, considerable efforts have been devoted to mimicking natural photoinduced electron transfer processes, such as those associated with the light-harvesting events in green plants that collect light energy for photosynthesis. Such natural photochemical functions in nanoscale devices and nanostructured materials are of prime importance in terms of applications in photovoltaics, organic light emitting diodes, photonics, and biomimetic light-harvesting.[1] In these fields, supramolecular organization of electron donor (**D**) and acceptor (**A**) molecules with controllable structural ordering has grown in interest, especially for the goal of developing high-performance devices such as field effect transistors (FETs) or organic solar cells.[2] To date, however, molecular-level and nanoscale ordered organization of **D** and **A** molecules within the functional molecular assemblies with well-defined shapes and structures still remains a challenge.[2]

Surfactant-templated mesoporous materials[3] have been envisaged as a platform for the next generation of functional materials by incorporation of optically active dye with diverse potential applications, such as sensors,[4] photoswitchable materials,[5] micrometer sized lasers or optical data storage,[6] drug delivery systems,[7] and so forth. Recently, porous materials have attracted considerable interest as hosts in electron and energy transfer

*Corresponding author. Fax: +86-10-6275-4179; E-mail: yan@pku.edu.cn.

(1) (a) Günes, S.; Neugebauer, H.; Sariciftci, N. S. *Chem. Rev.* **2007**, *107*, 1324. (b) Thompson, B. C.; Fréchet, J. M. J. *Angew. Chem., Int. Ed.* **2008**, *47*, 58.
(2) (a) Percec, V.; Glodde, M.; Bera, T. K.; Miura, Y.; Shiyanovskaya, I.; Singer, K. D.; Balagurusamy, V. S. K.; Heiney, P. A.; Schnell, I.; Rapp, A.; Spiess, H.-W.; Hudsonk, S. D.; Duank, H. *Nature* **2002**, *419*, 384. (b) Yamamoto, Y.; Fukushima, T.; Suna, Y.; Ishii, N.; Saeki, A.; Seki, S.; Tagawa, S.; Taniguchi, M.; Kawai, T.; Aida, T. *Science* **2006**, *314*, 1761.
(3) (a) Kresge, C. T.; Leonowicz, M. E.; Roth, W. J.; Vartuli, J. C.; Beck, J. S. *Nature* **1992**, *359*, 710. (b) Zhao, D.; Feng, J.; Huo, Q.; Melosh, N.; Fredrickson, G. H.; Chmelka, B. F.; Stucky, G. D. *Science* **1998**, *279*, 548. (c) Lu, A.-H.; Schüth, F. *Adv. Mater.* **2006**, *18*, 1793.
(4) (a) Fan, H.; Lu, Y.; Stump, A.; Reed, S. T.; Baer, T.; Schunk, R.; Perez-Luna, V.; López, G. P.; Brinker, C. J. *Nature* **2000**, *405*, 56. (b) Li, L.-L.; Fang, C.-J.; Sun, H.; Yan, C.-H. *Chem. Mater.* **2008**, *20*, 5977.
(5) (a) Liu, N.; Chen, Z.; Dunphy, D. R.; Jiang, Y.; Assink, R. A.; Brinker, C. J. *Angew. Chem., Int. Ed.* **2003**, *42*, 1731. (b) Liu, N.; Dunphy, D. R.; Atanassov, P.; Bunge, S. D.; Chen, Z.; López, G. P.; Boyle, T. J.; Brinker, C. J. *Nano. Lett.* **2004**, *4*, 551.
(6) (a) Marlow, F.; McGehee, M. D.; Zhao, D.; Chmelka, B. F.; Stucky, G. D. *Adv. Mater.* **1999**, *11*, 632. (b) Bartl, M. H.; Boettcher, S. W.; Hu, E. L.; Stucky, G. D. *J. Am. Chem. Soc.* **2004**, *126*, 10826. (c) Wang, J. F.; Stucky, G. D. *Adv. Funct. Mater.* **2004**, *14*, 409.
(7) (a) Nguyen, T. D.; Leung, K. C.-F.; Liong, M.; Liu, Y.; Stoddart, J. F.; Zink, J. I. *Adv. Funct. Mater.* **2007**, *17*, 2101. (b) Angelos, S.; Johansson, E.; Stoddart, J. F.; Zink, J. I. *Adv. Funct. Mater.* **2007**, *17*, 2261.

© 2009 American Chemical Society
Published on Web 09/18/2009

systems.[8−11] These host−guest materials could combine various functions of organic guests and the high stability of the silica framework, which not only serves to protect and stabilize the organic entities inside but also allow its optical properties to be probed from outside due to the chemical inertness and optical transparency of silica.[4−6] Several methods, mainly including postloading and cocondensation, have already been developed for inclusion of organic functional molecules into the mesopores.[12] With the developed pathways, the immobilization of lanthanide chelate complexes within mesostructured hosts has been achieved and received increased attention during the past decade for the fabrication of materials with tunable attributes offering modulated properties.[11] However, these methods often lead to a low loading and a random distribution of the organic groups within the host architecture. Highly doped mesostructured hybrids with ordered organization of guest species are desired for high-performance optical devices.[5]

Recently, self-assembly of amphiphilic molecules that can serve as both structure-directing agents (SDAs) and monomers seems to be one promising approach used for the fabrication of mesostructured functional nanocomposites.[13−17] Brinker and co-workers explored in situ polymerization using an amphiphilic diacetylenic surfactant as the structure-directing agent to template the formation of silica-type hybrid materials. The resulting polydiacetylene−silica composites exhibit interesting thermo-, solvato-, and mechano-chromatic properties.[13] Followed this pioneering work, the method has so far mainly been applied in inclusion of conjugated polymer chains in mesoporous channels. For example, surfactants containing pyrrole,[14] thiophene,[15,16] or poly(phenylene ethynylene)[17] have been recently synthesized and used as templates to prepare mesostructured polymer−silica nanocomposites. However, the functional surfactant directed synthesis of organic−inorganic hybrids that have structural ordering on the nanometer scale and that exhibit novel optical or electronic functionalities is less explored.[18−20] The Stupp group recently explored templating mesostructured silica-based hybrid materials using functional surfactants containing electronically active moieties.[18] The results indicate that the ordered and nanostructured environment leads to highly efficient energy transfer among organic components in these hybrid films. Most recently, the same group demonstrated a self-assembly of nonsilicate ordered hybrids with strongly interacting amphiphilic molecules containing optoelectronic functionality as structure-directing agent.[19] This biologically nontoxic hybrid contains lamellar polycrystalline ZnO separated by nanoscale layers of optoelectronic organic molecules, which attain stable and high photoconductive performance.

We have explored the utility of functional-template directed self-assembly approach in driving the orientational organization of small organic semiconductors within the periodic nanoscale silica channels.[20] Herein, to accomplish the goal of synthesizing hybrid nanostructures having both optoelectronic active organic and inorganic components,[19] we developed a novel hybrid organic−inorganic self-assembly approach to design and synthesize innovative donor−acceptor hybrid materials with intimately contacted nanoscale **D** and **A** domains organized in a three-dimensional ordering. Two specific organic and inorganic building blocks, both of which bear optoelectronic functions (potential **D** and **A**, respectively), were designed and used: one cationic surfactant, trimethyl-(10-anthracene-9-yl-decyl) ammonium bromide (TAAB), with a typical **D** moiety anthracene at the hydrophobic tail, was synthesized and used as the organic template (structure-directing agents); the silyilated viologen (SV) was used as both inorganic building blocks and **A** units. Then the one-step self-assembly process locks both **D** and **A** molecules into three-dimensional ordered nanostructure, which allows for the uniform and molecular level controllable organization of the **D** and **A** molecules and thus afford interesting optical behaviors. Furthermore, the nanostructured inorganic framework serves to protect, stabilize, and orient the **D** and **A** molecules and could provide sufficient mechanical

(8) (a) Nguyen, T. Q.; Wu, J.; Doan, V.; Schwartz, B. J.; Tolbert, S. H. *Science* **2000**, *288*, 652. (b) Nguyen, T. Q.; Wu, J.; Tolbert, S. H.; Schwartz, B. J. *Adv. Mater.* **2001**, *13*, 609.
(9) (a) Hernandez, R.; Franville, A. C.; Minoofar, P.; Dunn, B.; Zink, J. I. *J. Am. Chem. Soc.* **2001**, *123*, 1248. (b) Minoofar, P. N.; Hernandez, R.; Chia, S.; Dunn, B.; Zink, J. I.; Franville, A. C. *J. Am. Chem. Soc.* **2002**, *124*, 14388. (c) Minoofar, P. N.; Dunn, B.; Zink, J. I. *J. Am. Chem. Soc.* **2005**, *127*, 2656. (d) Johansson, E.; Zink, J. I. *J. Am. Chem. Soc.* **2007**, *129*, 14437.
(10) (a) Calzaferri, G.; Huber, S.; Maas, H.; Minkowski, C. *Angew. Chem., Int. Ed.* **2003**, *42*, 3732. (b) Maas, H.; Calzaferri, G. *Angew. Chem., Int. Ed.* **2002**, *41*, 2284. (c) Megelski, S.; Calzaferri, G. *Adv. Funct. Mater.* **2001**, *11*, 277. (d) Gfeller, N.; Calzaferri, G. *J. Phys. Chem. B* **1997**, *101*, 1396. (e) Ganschow, M.; Hellriegel, C.; Kneuper, E.; Wark, M.; Thiel, C.; Schulz-Ekloff, G.; Bräuchle, C.; Wöhrle, D. *Adv. Funct. Mater.* **2004**, *14*, 269.
(11) (a) Carlos, L. D.; Ferreira, R. A. S.; de Zea Bermudez, V.; Ribeiro, S. J. L. *Adv. Mater.* **2009**, *21*, 509. (b) Gago, S.; Fernandes, J. A.; Rainho, J. P.; Ferreira, R. A. S.; Pillinger, M.; Valente, A. A.; Santos, T. M.; Carlos, L. D.; Ribeiro-Claro, P. J. A.; Gonçalves, I. S. *Chem. Mater.* **2005**, *17*, 5077.
(12) (a) Hoffmann, F.; Cornelius, M.; Morell, J.; Fröba, M. *Angew. Chem., Int. Ed.* **2006**, *45*, 3216. (b) Schlossbauer, A.; Schaffert, D.; Kecht, J.; Wagner, E.; Bein, T. *J. Am. Chem. Soc.* **2008**, *130*, 12558. (c) Kecht, J.; Schlossbauer, A.; Bein, T. *Chem. Mater.* **2008**, *20*, 7207.
(13) (a) Lu, Y. F.; Yang, Y.; Sellinger, A.; Lu, M. C.; Huang, J. M.; Fan, H. Y.; Haddad, R.; Lopez, G.; Burns, A. R.; Sasaki, D. Y.; Shelnutt, J.; Brinker, C. J. *Nature* **2001**, *410*, 913. (b) Yang, Y.; Lu, Y. F.; Lu, M. C.; Huang, J. M.; Haddad, R.; Xomeritakis, G.; Liu, N. G.; Malanoski, A. P.; Sturmayr, D.; Fan, H. Y.; Sasaki, D. Y.; Assink, R. A.; Shelnutt, J. A.; van Swol, F.; Lopez, G. P.; Burns, A. R.; Brinker, C. J. *J. Am. Chem. Soc.* **2003**, *125*, 1269. (c) Peng, H. S.; Tang, J.; Pang, J. B.; Chen, D. Y.; Yang, L.; Ashbaugh, H. S.; Brinker, C. J.; Yang, Z. Z.; Lu, Y. F. *J. Am. Chem. Soc.* **2005**, *127*, 12782.
(14) Ikegame, M.; Tajima, K.; Aida, T. *Angew. Chem., Int. Ed.* **2003**, *42*, 2154.
(15) Li, G.; Bhosale, S.; Wang, T.; Zhang, Y.; Zhu, H.; Fuhrhop, J.-H. *Angew. Chem., Int. Ed.* **2003**, *42*, 3818.
(16) Yang, Z.; Kou, X.; Ni, W.; Sun, Z.; Li, L.; Wang, J. F. *Chem. Mater.* **2007**, *19*, 6222.
(17) Clark, A. P.-Z.; Shen, K. F.; Rubin, Y. F.; Tolbert, S. H. *Nano. Lett.* **2005**, *5*, 1647.
(18) (a) Tajima, K.; Li, L.-S.; Stupp, S. I. *J. Am. Chem. Soc.* **2006**, *128*, 5488. (b) Sofos, M.; Stone, D. A.; Goswami, D. K.; Okasinski, J. S.; Jin, H.; Bedzyk, M. J.; Stupp, S. I. *J. Phys. Chem. C* **2008**, *112*, 2881.
(19) Sofos, M.; Goldberger, J.; Stone, D. A.; Allen, J. E.; Ma, Q.; Herman, D. J.; Tsai, W.-W.; Lauhon, L. J.; Stupp, S. I. *Nat. Mater.* **2009**, *8*, 68.
(20) Li, L.-L.; Sun, H.; Bai, Y.-C.; Fang, C.-J.; Yan, C.-H. *Chem.—Eur. J.* **2009**, *15*, 4716.

Scheme 1. Synthetic Procedures of the Two Functional Self-Assembling Building Blocks[a]

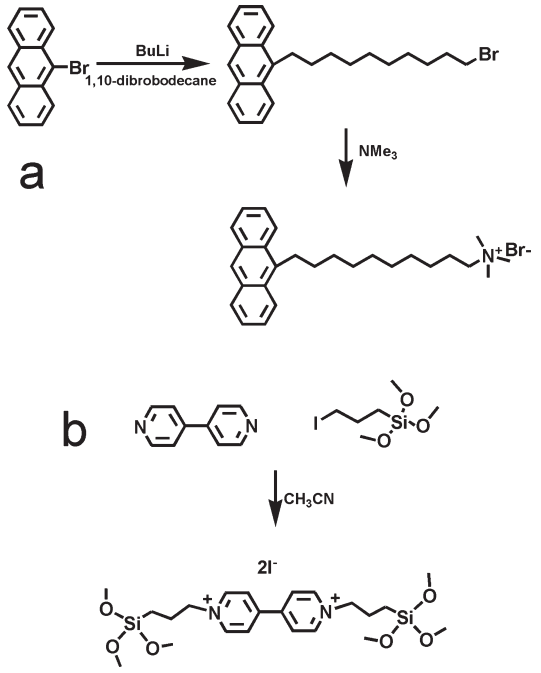

[a] (a) The cationic surfactant, trimethyl-(10-anthracene-9-yl-decyl) ammonium bromide (TAAB), with a special electron donor moiety anthracene at the hydrophobic tail; (b) the silyilated viologen (SV) as both electron acceptor unit and silica source.

and chemical stability to enable integration of **D**/**A** blends into devices and microsystems.

Experimental Section

Materials. All chemicals were of reagent grade and were used without further purification unless otherwise noted. Tetraethyl orthosilicate (TEOS) and ammonia (28 wt %) were obtained from Beijing Chemical Reagent Company.

Synthesis. The anthracene containing surfactant (TAAB) was synthesized as in previous work, which has been proven to direct the self-assembly of silica mesophases.[20] First, 9-(10-bromodecyl)anthracene was synthesized by treating 9-bromoanthracene with *n*-BuLi in THF and quenching the 9-lithio-anthracene with 1,10-dibromodecane. Then the cationic ammonium surfactants (TAAB) that have anthracene at the ends of their hydrophobic tails were obtained by the reaction of trimethylamine with the bromodecyl-terminated anthracene in alcoholic solutions (Scheme 1a). Viologen is a typical electron acceptor unit, which has been widely used in a variety of electron transfer systems. The silyilated viologen (SV) was prepared through the attachment of trimethoxysilylpropyl groups to the nitrogen atoms of 4,4′-bipyridine by nucleophilic substitution (Scheme 1b).[21]

The synthesis of mesostructured hybrids was started by mixing calculated amounts of the structure-directing agents (a costructure-directing agents of TAAB/CTAB = 1:9 or TAAB only, respectively), distilled water, and concentrated NH_4OH (28%). The mixture was stirred until the surfactants were completely dissolved. The silica precursors, TEOS and SV (dissolved in minimum distilled water) with different molar fractions (SV/TEOS = 0:100 (SVAT0, SVA0), 6:94 (SVAT6, SVA6), and 10:90 (SVAT10, SVA10) based on Si contribution), were then added at a molar ratio of 1.0 Si:114 H_2O:8.0 NH_4OH (28%):0.12 structure-directing agents. The resulting solution was stirred at room temperature for 30 min and then transferred to a polyethylene bottle. The bottle was closed and kept in an isothermal oven at 90 °C for 5 h. During this period of time, particles were observed to form and precipitate at the bottom of the bottle. They were isolated and washed thoroughly with distilled water. The sample was dried in vacuum at room temperature. Elemental analysis. SVAT0: C 27.94, H 5.52, N 1.68%. SVAT6: C 30.11, H 5.80, N 2.01%. SVAT10: C 29.99, H 5.67, N 2.16%. SVA0: C 35.78, H 4.97, N 1.60%. SVA6: C 34.41, H 4.68, N 1.76%. SVA10: C 36.24, H 4.86, N 2.02%.

Characterization. X-ray powder diffraction (XRD) patterns of the nanocomposite particles were recorded on a Rigaku Dmax-2000 X-ray powder diffractometer (Japan) using Cu Kα (λ = 1.5405 Å) radiation. TEM images were taken on the Hitachi H-9000 NAR transmission electron microscope under a working voltage of 300 kV. Elemental analyses (C, H, N) were performed on an Elementar Vario EL analyzer. Proton-decoupled ^{29}Si MAS NMR spectra were recorded on a Varian-Unity INOVA 300 MHz spectrometer operating at 59.624 MHz (1.5 ms pulse width, 5000 transients, spin speed 6 kHz, acquisition time 0.02 s, pulse delay 3 s). UV/vis spectra were recorded on a Shimadzu UV-3100 spectrometer equipped with a diffuse reflectance accessory and using $BaSO_4$ as reference. The fluorescence spectra were recorded on a Hitachi F-4500 fluorescence spectrophotometer. Time-resolved fluorescence spectra were obtained using an Edinburgh FLS920 fluorescence spectrophotometer. The instrument was operated with a thyratron-gated flash lamp filled with hydrogen at a pressure of 0.5 atm. The lamp was operated at a frequency of 40 kHz, and the pulse width of the lamp under operating conditions was about 1.2 ns. The lifetimes were estimated from the measured fluorescence decay curves and the lamp profile using a nonlinear least-squares iterative fitting procedure.

Results and Discussion

Functional Building Blocks Design and Self-Assembly Process. Self-assembly is emerging as one of the most promising approaches toward the fabrication of smart materials with designed structures and functions. Nature has given us many such elegant examples constructed by the self-assembly processes. Similar to building a machine from parts, a self-assembly process comes from special molecular building blocks. Herein, two functional self-assembling building blocks carrying potential electron donor (anthracene) and electron acceptor (viologen), respectively, were designed and synthesized (Scheme 1). As shown schematically in Scheme 2, the **D**-containing cationic surfactants TAAB were used as structure-directing agents (SDAs) to prepare the mesostructured hybrid in a one-phase route under strong basic conditions. And the silyilated viologen (SV) and tetraethyl orthosilicate (TEOS) were used as the silica precursor. The formation mechanism of the hybrids is dictated by two features.[12a,22−24] The first

(21) (a) Álvaro, M.; Ferrer, B.; Fornés, V.; García, H. *Chem. Commun.* **2001**, 2546. (b) Díaz, U.; Cantín, Á.; Corma, A. *Chem. Mater.* **2007**, *19*, 3686.

(22) (a) Attard, G. S.; Glyde, J. C.; Göltner, C. G. *Nature* **1995**, *378*, 366. (b) Kickelbick, G. *Angew. Chem., Int. Ed.* **2004**, *43*, 3102.

(23) (a) Huo, Q.; Margolese, D. I.; Ciesla, U.; Feng, P.; Gier, T. E.; Sieger, P.; Leon, R.; Petroff, P. M.; Schüth, F.; Stucky, G. D. *Nature* **1994**, *368*, 317. (b) Huo, Q.; Margolese, D. I.; Ciesla, U.; Demuth, D. G.; Feng, P.; Gier, T. E.; Sieger, P.; Firouzi, A.; Chmelka, B. F.; Schüth, F.; Stucky, G. D. *Chem. Mater.* **1994**, *6*, 1176.

Scheme 2. Molecular Structural Characteristic of the Two Self-Assembling Building Blocks (left), Hierarchical Self-Assembly Process (middle), and the Representative Structure of the Donor−Acceptor Hybrids with Molecular-Scale and Mesoscale Segregation and Ordering (right)

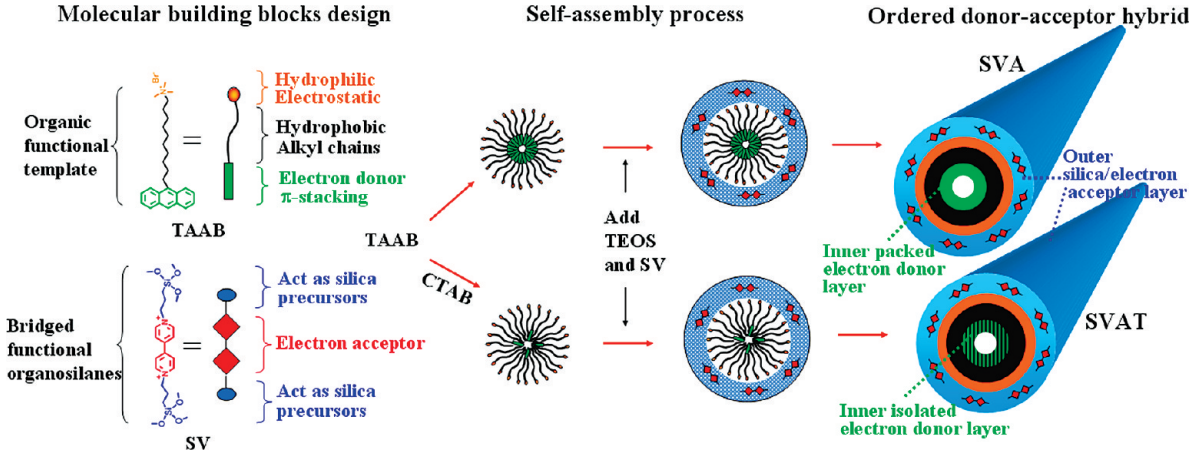

is that surfactant molecules (SDAs) form molecular assemblies which lead to micelle and, ultimately, liquid crystal formation. The second is the condensation of silica precursors (both TEOS and SV) around the surfactants and thus formation of the final continuous framework owing to the counterion interactions and confined growth.[23] Thus, the photoelectron donor (anthracene) that was attached at the ends of the hydrophobic tails of the SDAs can be controllably driven into the central regions of the pore channels. The photoelectron acceptor (viologen) was covalently incorporated in/on the pore walls through the hydrolysis−condensation of SV with co-condensable alkoxysilane arms and TEOS. Several below features of such a hierarchical self-assembly strategy make it particularly attractive for the development of optoelectronic materials. (1) The one-step organic−inorganic self-assembly process leads to ordered materials with molecular-scale and mesoscale distinguishable segregation of different functional groups (**D** and **A** in this case) within the channel pores and walls, respectively, which exemplify the enormous potential of self-assembly for the construction of well-defined nanostructures by controlling the molecular building blocks. (2) The symmetry of the self-assembly architecture guarantees not only a high loading but also an orientational organization of **D** groups within the central regions of the pore channels for hybrids SVA; such a dense packing is highly important in control of the direction and efficiency of electron or energy transfer. Furthermore, the loading content of the **D** groups, intermolecular **D**−**D** interactions, and further the optical properties of the composites can be modulated (for hybrids SVAT) by using conventional ammonium surfactants (CTAB) as the costructure-directing agents for tailoring the self-assembly process (Scheme 2). Since the length and amphiphilic structure of functional template TAAB is similar to that of a CTAB molecule, the TAAB could distribute homogeneously into CTAB micelles when the mesostructured hybrid is formed. Thus, the functional surfactant TAAB molecules could be well isolated by CTAB molecules. It is because the amount of TAAB is minor relative to CTAB, and further electrostatic repulsion and packing frustration could separate any chains that assemble into the same domain. This placement is an example of the "philicity" strategy.[9d,14,17] (3) It has been demonstrated that the organic bridging groups (−R−) could be densely and covalently embedded within the pore walls in the periodic mesoporous organosilicas (PMOs) synthesized with the precursors of organic-bridged alkoxysilane $(R'O)_3Si-R-Si(OR')_3$.[24] Due to this feature, many works have reported on the incorporation of interactive bridging organic groups that carry adsorbent, optical, electronic, chiral, and catalytic functions within the silica pore walls.[12a,25] Interestingly, the novel hierarchical self-assembly approach we demonstrate here can be conjured as the ideal of functional-template (TAAB) directed synthesis of the innovative PMOs, where **A** (viologen)-bridged alkoxysilane precursors (SV) were used. Obviously, this leads us to infer that it should readily be possible to substitute the **D** and **A** for alternative different functional groups, with a concomitant possibility to rationally tailor the physical and chemical properties of both the pores and walls of mesostructured materials.

Structure Characterization. Low angle XRD patterns (Figure 1) show that both the two series of hybrids SVA and SVAT retain the two-dimensional hexagonal structure, with three well-resolved peaks indexed as (100), (110), and (200) reflection planes of the hexagonal space group *p6mm*. The d_{100} values with a slight fluctuation (3.8−4.2 nm) can be deduced. The gradually incorporation of SV induces a decrease in the XRD peak intensities. However, the three Bragg peaks are still observed for the hybrids SVAT(0,6,10) and SVA(0,6), indicating that the

(24) (a) Asefa, T.; MacLachlan, M. J.; Coombs, N.; Ozin, G. A. *Nature* **1999**, *402*, 867. (b) Inagaki, S.; Guan, S.; Fukushima, Y.; Oshuna, T.; Terasaki, O. *J. Am. Chem. Soc.* **1999**, *121*, 9611. (c) Melde, B. J.; Holland, B. T.; Blanford, C. F.; Stein, A. *Chem. Mater.* **1999**, *11*, 3302. (d) Inagaki, S.; Guan, S.; Ohsuna, T.; Terasaki, O. *Nature* **2002**, *416*, 304.

(25) (a) Alvaro, M.; Benitez, M.; Das, D.; Garcia, H.; Peris, E. *Chem. Mater.* **2005**, *17*, 4958. (b) Corriu, R. J. P.; Mehdi, A.; Reyé, C. *J. Mater. Chem.* **2005**, *15*, 4285. (c) Hunks, W. J.; Ozin, G. A. *J. Mater. Chem.* **2005**, *15*, 3716. (d) Fujita, S.; Inagaki, S. *Chem. Mater.* **2008**, *20*, 891.

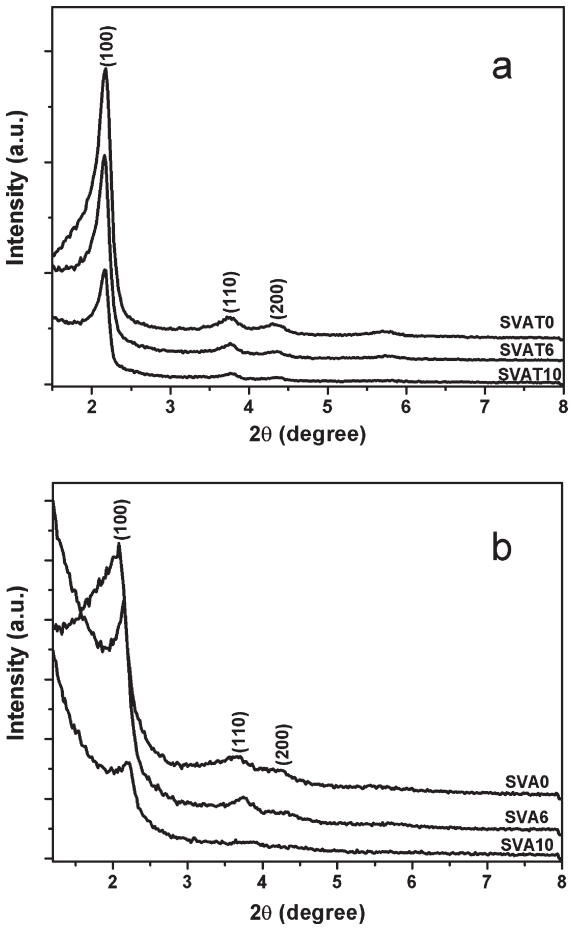

Figure 1. Small-angle XRD patterns of the two series of donor−acceptor hybrids (a) SVAT and (b) SVA with increasing proportions of SV.

hexagonal symmetry of the materials was preserved. The attenuation of the XRD peaks is probably due to a reduction in the X-ray scattering contrast between the silica walls and pore-filling material[26] or a gradual loss of structural order. For SVA10, the (100) peak is notably broadened and the (110) and (200) reflections almost disappear, suggesting a much lower structural regularity of the silica matrix, which was confirmed by the transmission electron microscopy (TEM) images (see below). These changes in X-ray diffraction profiles are in accordance with results previously described for PMO materials.[27]

The TEM images (Figure 2, Figure S1 in Supporting Information) also confirm that the hexagonal mesostructure is maintained with the incorporation of SV unit in the mesostructure. Both the hybrids SVAT6 and SVA6 display hexagonally arranged channels throughout the sample with a center to center distance between the hexagon centers of 3.6−4.0 nm, which is comparable with the XRD results. While increasing the amount of incorporated SV moiety, regularly aligned hexagonal channels are clearly seen in the TEM images of the hybrids SVAT10. However, a deteriorated patterned mesostructure is observed for the hybrids SVA10, demonstrating a less-ordered phase. From the highly ordered architecture of the composite materials, we further confirm that the **D** and **A** molecules are uniformly organized into precise three-dimensional arrangements.

Regarding the organization of the TAAB and SV units within the channel pores and walls of the assemblies, respectively, FTIR analyses were obtained for the accurate characterization of the hybrid materials. Figure 3 and Figure S2 (see Supporting Information) depict the FTIR spectra recorded at 1750−1350 and 4000−600 cm^{-1}, respectively, for the starting self-assembling building blocks used in the synthesis of the periodical hybrid materials as well as the final mesostructures. All the hybrids presented characteristic bands for aliphatic C−H stretching vibrations of alkyl chains around 2990−2810 cm^{-1} and a strong band at 1350−870 cm^{-1} due to the stretching vibrations of the Si−OH and Si−O−Si frameworks. The band at approximately 1485 cm^{-1} was assigned to C=C stretching vibrations of the anthracene functional groups. All of the synthesized mesostructures show very similar IR spectra with differences only in the relative intensities of the characteristic SV band at 1650 cm^{-1}. Increasing amount of SV used leads to increased absorption intensity. As shown in Figure 3, the discernible peaks at 1650 cm^{-1} for both mesostructures SVAT (templated from a mixture of TAAB and CTAB) and SVA (directed from TAAB only) gradually attenuate with decreasing organic contents SV.

Another piece of evidence of the building blocks SV covalently bonded into the porous walls is obtained by solid-state ^{29}Si NMR (Figure 4). The spectra of the hybrids displayed two regions of major peaks, centered at about −85 to −120 and about −70 ppm. These two regions correspond to $Si(-O-)_4$ (Q groups) and $RSi(-O-)_3$ (T groups) species, respectively, where R is the viologen organic group. The deconvolution of the ^{29}Si NMR spectra was obtained for the quantification of the species associated with the respective peaks. The mesostructures formed without addition of SV showed three peaks at −110, −98, and −88 ppm, assigned to Q^4 framework silica sites ($Si(OSi)_4$), Q^3 silanol sites ($Si(OSi)_3OH$), and Q^2 silanol sites $(Si(OSi)_2)(OH)_2$, respectively. For the mesostructures with appropriate loading of SV, a lower-shielding pattern is formed with one broad convoluted peak, which is composed of one major peak at about −68 ppm, corresponding to $RSi(OSi)_2OH$ (T^2) species, and two shoulders at about −61 ppm and −72 ppm due to the species $RSi(OSi)(OH)_2$ (T^1) and $RSi(OSi)_3$ (T^3), respectively. This result indicates the presence of Si atoms covalently bonded to carbon atoms, confirming the presence of organic functionalities viologen embeded into the final materials.[27]

It is well-known that the cationic surfactants, which were entrapped in channels through the electrostatic interaction between the electropositive group of the surfactant and the silicate walls, can be washed out.

(26) (a) Fu, L.; Ferreira, R. A. S.; Valente, A.; Rocha, J.; Carlos, L. D. *Microporous Mesoporous Mater.* **2006**, *94*, 185. (b) Hammond, W.; Prouzet, E.; Mahanti, S. D.; Pinnavaia, T. J. *Microporous Mesoporous Mater.* **1999**, *27*, 19.

(27) (a) Wahab, M. A.; Hussain, H.; He, C. *Langmuir* **2009**, *25*, 4743. (b) García, R. A.; van Grieken, R.; Iglesias, J.; Morales, V.; Gordillo, D. *Chem. Mater.* **2008**, *20*, 2964.

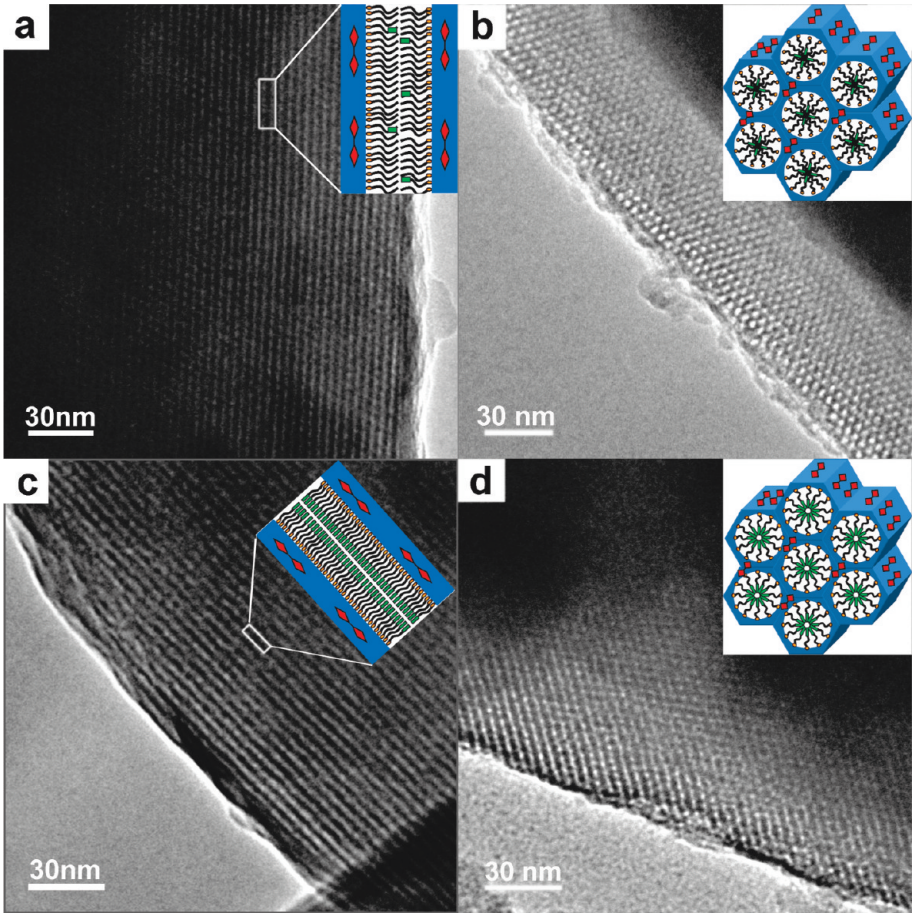

Figure 2. TEM images of the donor−acceptor hybrids SVAT6 recorded (a) in the direction perpendicular to the pore axis and (b) in the direction of the pore axis and of the donor−acceptor hybrids SVA6 recorded (c) in the direction perpendicular to the pore axis and (d) in the direction of the pore axis. Insets show the schematic representations of the locally ordered structure on molecular- and meso-scale.

The ordered structure of the nanocomposites was further confirmed by the acid/ethanol extraction of the hybrids SVAT6 and SVA6 to remove the functional surfactants and generate mesoporosity (Figure 5). The XRD patterns of the extracted samples (Figure S3 in Supporting Information) showed that the highly ordered hexagonal structure was retained. Figure 5b,c shows the N_2 adsorption−desorption isotherms as well as the pore size distribution for the extracted samples. Both the materials show nitrogen adsorption−desorption curves lying in the group of type IV isotherms, according to the IUPAC classification, typical for mesoporous solids. The steep region detected in the adsorption branch around $P/P_0 = 0.32$, corresponding to the capillary condensation of nitrogen in uniform pores. Furthermore, the Barrett−Joyner−Halenda (BJH) analysis shows a special Brunauer−Emmett−Teller (BET) surface area of 740 and 704 m^2/g for extracted SVAT6 and SVA6 samples, respectively; which is evidence of the formation of well-structured mesoporous materials. This conclusion is also supported by the quite narrow pore size distribution calculated from the adsorption isotherm for these materials. The pore diameter (2.6 and 2.9 nm for extracted SVAT6 and SVA6 samples, respectively) agreed well with that deduced from TEM and XRD results. The value of 2.9 nm for SVA6 is close to the diameter of a single rod micelle of TAAB surfactants. A slightly different pore diameter of 2.6 nm was expected for SVAT6 that was directed by the composite surfactants of TAAB and CTAB, since the cationic−cationic mixed surfactant could influence the micelle formation. Furthermore, the wall thickness is estimated to be about 1.0−1.5 nm from XRD and nitrogen physisorption results. The UV/vis spectra (Figure S4 in Supporting Information) of the extracted samples show an intense band around 270 nm for the viologen unit,[21] which further confirms that the organic bridging groups (−viologen−) are covalently bonded in the porous walls.

Optical Properties. The optical properties were investigated by measuring the photoluminescence (PL) spectra of the series of samples with different ratios of anthracene to viologen. Typical spectra for the assemblies are presented in Figure 6. The hybrid SVAT series demonstrates the characteristics of anthracene monomer emission centered at 420 nm with resolvable vibrational fine structure,[28] since the TAAB are fairly isolated within the pore channels by CTAB molecules. In contrast, the mesostructures SVA exhibited a broad and structureless emission band with a maximum at 470 nm, which results from

(28) Zhang, G.; Yang, G.; Wang, S.; Chen, Q.; Ma, J. S. *Chem.—Eur. J.* **2007**, *13*, 3630.

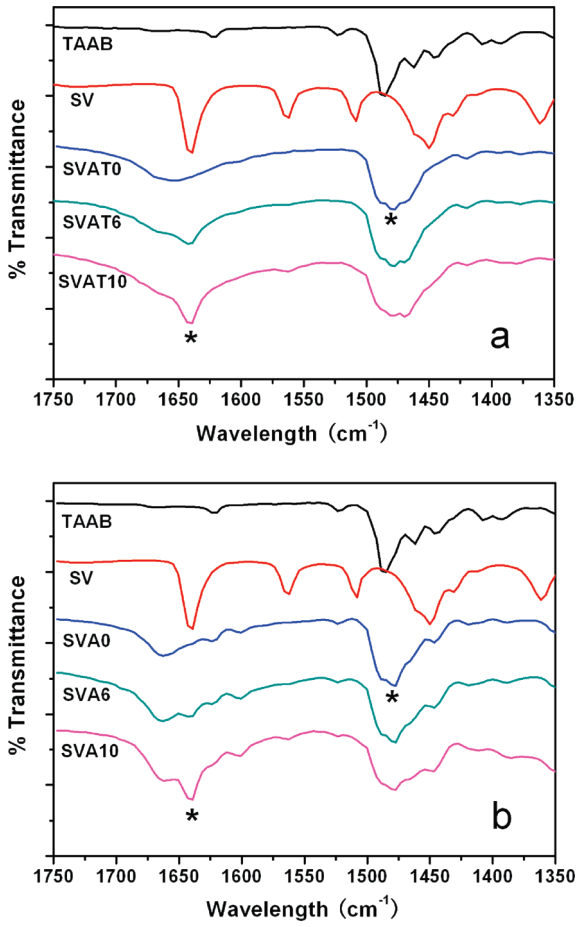

Figure 3. FT-IR spectra of the starting self-assembling building blocks TAAB and SV used in the synthesis as well as the two series of donor−acceptor hybrids (a) SVAT and (b) SVA with increasing proportions of SV.

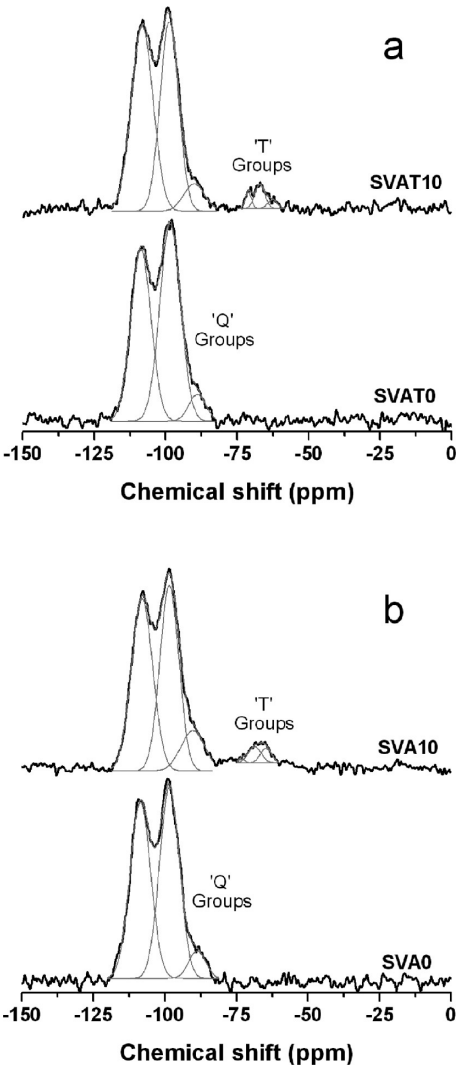

Figure 4. ^{29}Si MAS NMR spectra of the donor−acceptor hybrids: (a) SVAT0 and SVAT10; (b) SVA0 and SVA10.

a large overlap between the anthracene moieties and thus the formation of intermolecular excimer.[29] The anthracene groups are packed together in the central regions of the pore channels of the mesostructures SVA. The dense packing of the anthracene groups permits their neighboring planar aromatic surface to achieve extensive intermolecular $\pi-\pi$ interactions and thus to form excimer.[20] This further confirms that the self-assembling strategy we demonstrated here not only guarantees a periodical organization of the different functionalities (**D** and **A**, in this case), but also allows for the molecular level controllable modulation of the **D**−**D** interactions within the pore channels upon tailoring the self-assembly process. It is interesting to note that as SV is gradually introduced into the SVAT and SVA hybrid materials, both emissions of the monomer and excimer of anthracene can be gradually quenched. Fluorescence quenching could come from energy or electron transfer between donor and acceptor.[30] In general, efficient energy transfer requires good spectra overlap between the acceptor absorption and the donor emission spectra. For the quencher SV in our systems, its absorption spectrum overlaps less with the emission spectra of anthracene monomer and that of excimer (Figure S5 in Supporting Information). Since this overlap is not efficient enough, the intermolecular energy transfer from anthracene to viologen could not be the main reason for quenching of the fluorescence emissions.

Moreover, it is well-known that anthracene and alkyl viologens are typical **D**/**A** pairs and fluorescence of anthracene and their derivatives can be quenched by alkyl viologens through a photoinduced electron transfer (PET) mechanism.[31] To further confirm the occurrence of electron transfer in our systems, the fluorescence decay curves were measured for the electron donor in the presence of varied amounts of the electron acceptor (Figure 7). The fluorescence decay of the composite SVAT0 is well fitted to a monoexponential profile with the lifetime of approximately 5.6 ns, which reflects the decay of the locally excited anthracene (monomer).[32]

(29) (a) Amicangelo, J. C.; Leenstra, W. R. *J. Am. Chem. Soc.* **2003**, *125*, 14698. (b) Kaanumalle, L. S.; Gibb, C. L. D.; Gibb, B. C.; Ramamurthy, V. *J. Am. Chem. Soc.* **2005**, *127*, 3674. (c) Mizobe, Y.; Miyata, M.; Hisaki, I.; Hasegawa, Y.; Tohnai, N. *Org. Lett.* **2006**, *8*, 4295.
(30) Liu, B.; Bazan, G. C. *J. Am. Chem. Soc.* **2006**, *128*, 1188.
(31) (a) Gong, Y.-K.; Miyamoto, T.; Nakashima, K.; Hashimoto, S. *J. Phys. Chem. B* **2000**, *104*, 5772. (b) Gong, Y.-K.; Nakashima, K. *J. Phys. Chem. B* **2002**, *106*, 803. (c) Hsiao, J.-S.; Eckert, A. R.; Webber, S. E. *J. Phys. Chem.* **1994**, *98*, 12032.
(32) Zhang, X.; Sasaki, K.; Kuroda, Y. *J. Org. Chem.* **2006**, *71*, 4872.

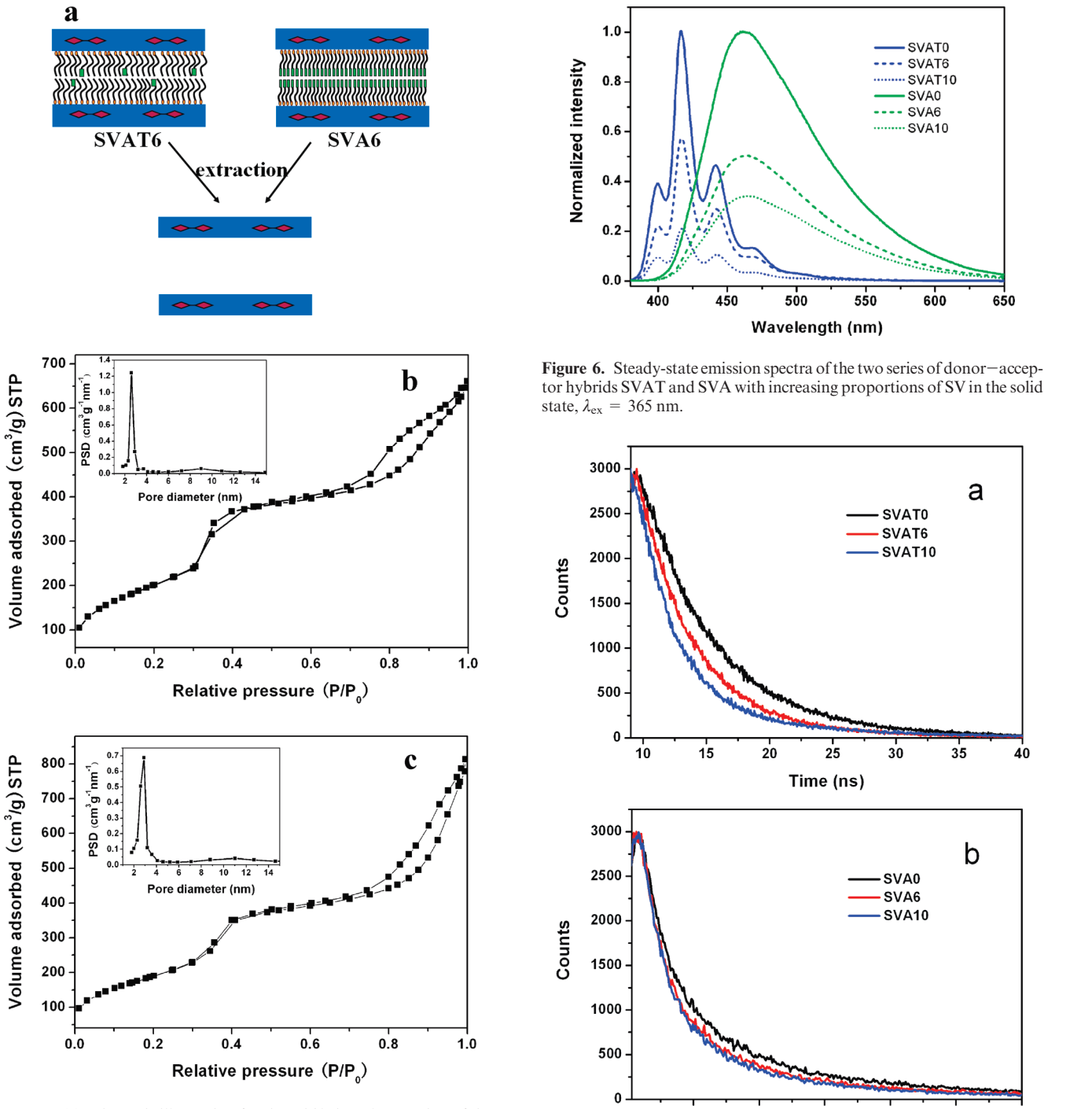

Figure 5. (a) Schematic illustration for the acid/ethanol extraction of the hybrids SVAT6 and SVA6 to remove the functional surfactants and generate mesoporosity. Nitrogen adsorption−desorption isotherms of (b) the extracted SVAT6 sample and (c) extracted SVA6 sample (Insets: corresponding pore size distributions for the extracted samples).

Incorporation of SV into the mesostructure to form the nanohybrids accelerated the anthracene monomer fluorescence decay. The anthracene-fluorescence lifetimes evaluated under these conditions were found to be 4.5 and 3.5 ns for the SVAT6 and SVAT10, respectively. In contrast, the observation of a second long decay component in the excited state lifetimes (13.4 ns, 62%; 2.9 ns, 38%) corroborates the existence of an emissive excimer

Figure 6. Steady-state emission spectra of the two series of donor−acceptor hybrids SVAT and SVA with increasing proportions of SV in the solid state, λ_{ex} = 365 nm.

Figure 7. Fluorescence decay profiles of the two series of donor−acceptor hybrids: (a) SVAT and (b) SVA in the solid state monitored at their maximum emission wavelength, λ_{ex} = 365 nm.

for the hybrids SVA0, in which the shorter decay parameter is attributed to the emission of the monomer of anthracene.[20,33] It turned out that increased incorporation of SV also accelerated this biexponential fluorescence decay (Table S1 in Supporting Information). Thus, the electron transfer is further verified by observing the decrease in fluorescence lifetime as the acceptor proportion is increased.[9d,31] It is reasonable to deduce that this electron transfer would not only directly quench the

(33) Molard, Y.; Bassani, D. M.; Desvergne, J.-P.; Moran, N.; Tucker, J. H. R. *J. Org. Chem.* **2006**, *71*, 8523.

Scheme 3. Possible Binding Model of the Viologen Groups in the Mesostructured Hybrid (left), Which Are Not Only Buried in the Pore Walls (a) but Also Anchored in the Pore Channels (b and c) and Molecular Representation of the Silylated Viologen Used in the Synthesis (right)

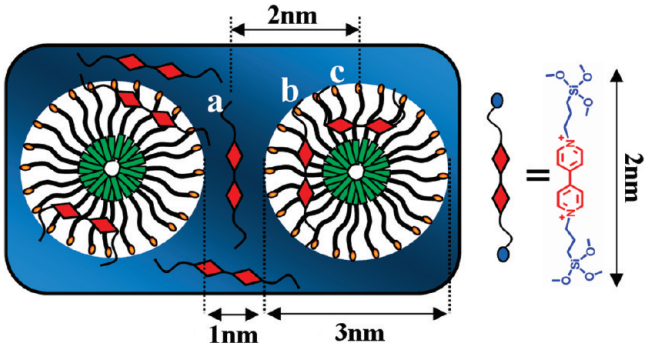

anthracene monomer emission but also hinder the excimer formation and thus quench their emission, since the excimer formation requires the encounter of one electronically excited fluorophore with another, usually that of the ground state, in an extremely short time.[34] Most recently, Chen and Krastev[35] described that an anionic pyrene derivative and a cationic poly(allyamine hydrochloride) self-aggregate to nanoparticles, where the confinement of pyrene molecules results in the fluorescence of excimer. And a quencher of 9,10-anthraquinone-2,6-disulfonic acid not only quenches pyrene monomer fluorescence but also leads to an efficient quenching of this excimer fluorescence. Through a similar pathway, the SVA system where anthracene packed densely within the central regions of the pore channels can be regarded as a pseudoconjugated system, where the excitons should be partially delocalized and can easily diffuse to the quencher association sites and result in the quenching.[35]

We are motivated to disclose the quenching of TAAB fluorescence by SV in our hybrid systems, which can provide an effective means to examine the distribution model of SV within the mesostructured hybrids. The length occupied by the bridged viologen (SV) is calculated to be 2 nm.[21b] Taking into account the pore diameter (about 3 nm) and wall thickness (about 1 nm), the distance between anthracene and viologen would be about 1−2 nm if the SV was fully buried within the silica framework (Scheme 3a), which would be proper for energy transfer but too long for effective electron transfer.[9] This predicates a different distribution model of SV within the mesostructure. Mercieret et al. have described that lypophilic interactions between the organosilane molecules and the hydrophobic core of the micelles could result in the deeper penetration of the organosilane molecules within the micelle than do the TEOS molecules.[36] Similar incorporation of the bridged organic molecules within the pore channels have also been reported by other authors for the synthesis of PMOs.[27,37] On the basis of these previous results, it is rational to conclude that the observed electron transfer behavior in our system is mostly due to the contrast matching between the silicate framework and organic moieties which are not only bridged in the silica framework (Scheme 3a) but also anchored in the pore channels (Scheme 3b,c, thus could lead to much more close distance between anthracene and viologen). In this study, it is very plausible that the loading of SV could affect micelle formation for mesophases, since SV contains π-functional and flexible larger groups which could approach themselves slowly at the interface of organosilicate/surfactant micelles. This will cause the micelle structure to "open-up" and allow functional silane molecules to migrate deeper within the micelle, where the silylated viologens were anchored covalently to the pore walls through a subsequent cross-linking co-condensation process.[27a] Furthermore, in this system, since both the anthracene (at the hydrophobic tail of the surfactant and thus in the central regions of micelle structure) and the silylated viologen are conjugated aromatics, the intermolecular $\pi-\pi$ interactions between them may also contribute to the migration of SV within pore channels. In this hierarchical self-assembly approach, the length of the chain linker of the anthracene containing surfactant (TAAB) could be shortened to improve the electron transfer efficiency. Obviously, this hierarchical self-assembly approach is promising to construct effective energy transfer systems through simple organic synthesis to substitute the anthracene and viologen for alternative different donor and acceptor groups to realize a strong overlap between the acceptor absorption and the donor emission spectra.

Conclusions

We have developed a novel one-step hybrid organic−inorganic self-assembly approach for the fabrication of hierarchically mesostructured materials with controllable organization of different optoelectronic functionalities in a three-dimensional ordering. It was demonstrated that this hybrid organic−inorganic design can be a rational strategy for the spontaneous formation of molecularly engineered optoelectronic materials with segregated donor−acceptor geometries. This work has opened a new window in designing an efficient synthesis protocol for molecular building blocks and in controlling their self-assembled superstructures of both theoretical and practical interest. We believe this research can offer an efficient molecular design and assembly methodology to fabricate a family of optoelectronic materials applicable in FETs, solar cells, and so forth.

Acknowledgment. The authors gratefully acknowledge financial aid from NSFC (20821091 and 20771009) and the Beijing Natural Science Foundation (Grant 2082007).

Supporting Information Available: Additional figures and table (PDF). This material is available free of charge via the Internet at http://pubs.acs.org.

(34) Chiba, J.; Takeshima, S.; Mishima, K.; Maeda, H.; Nanai, Y.; Mizuno, K.; Inouye, M. *Chem.—Eur. J.* **2007**, *13*, 8124.
(35) Chen, J.; Dong, W.; Möhwald, H.; Krastev, R. *Chem. Mater.* **2008**, *20*, 1664.
(36) Richer, R.; Mercier, L. *Chem. Commun.* **1998**, 1775.
(37) Gao, L.; Wei, F.; Zhou, Y.; Fan, X. X.; Wang, Y.; Zhu, J. H. *Chem.—Eur. J.* **2009**, *15*, 8310.